We are IntechOpen, the world's leading publisher of Open Access books Built by scientists, for scientists

6,900
Open access books available

185,000
International authors and editors

200M
Downloads

154
Countries delivered to

Our authors are among the

TOP 1%
most cited scientists

12.2%
Contributors from top 500 universities

BOOK CITATION INDEX
CLARIVATE ANALYTICS
INDEXED

WEB OF SCIENCE™

Selection of our books indexed in the Book Citation Index
in Web of Science™ Core Collection (BKCI)

Interested in publishing with us?
Contact book.department@intechopen.com

Numbers displayed above are based on latest data collected.
For more information visit www.intechopen.com

Chapter

Investigation of Zn/Ni-Based Electrocatalysts for Electrochemical Conversion of CO_2 to SYNGAS

Mohammadali Beheshti, Saeid Kakooei,
Mokhtar Che Ismail and Shohreh Shahrestani

Abstract

In the last decade, there is some research on the conversion of CO_2 to energy form. CO_2 can be converted to value-added chemicals including HCOOH, CO, CH_4, C_2H_4, and liquid hydrocarbons that can be used in various industries. Among the methods, electrochemical methods are of concern regarding their capability to operate with an acceptable reaction rate and great efficiency at room temperature and can be easily coupled with renewable energy sources. Besides, electrochemical cell devices have been manufactured in a variety of sizes, from portable to large-scale applications. Catalysts that optionally reduce CO_2 at low potential are required. Therefore, choosing a suitable electrocatalyst is very important. This chapter focused on the electrochemical reduction of CO_2 by Zn-Ni bimetallic electrocatalyst. The Zn-Ni coatings were deposited on the low-carbon steel substrate. Electrochemical deposition parameters such as temperature in terms of LPR corrosion rate, microstructure, microcracks, and its composition have been investigated. Then, the electrocatalyst stability and activity, as well as gas intensity and selectivity, were inspected by SEM/EDX analysis, GC, and electrochemical tests. Among the electrocatalysts for CO_2 reduction reaction, the $Zn_{65\%}-Ni_{35\%}$ electrode with cluster-like microstructure had the best performance for CO_2 reduction reaction according to minimum coke formation (<10%) and optimum CO and H_2 faradaic efficiencies (CO FE% = 55% and H2 FE% = 45%).

Keywords: electrocatalyst, electrochemical method, CO_2 reduction reaction, Zn-Ni, energy conversion, pollution, catalyst activity and stability

1. Introduction

Carbon dioxide is a chemical compound made up of one carbon atom and two oxygen atoms. It is existing in minimal concentrations in the atmosphere and behaves as a greenhouse gas that promotes environmental warming and pollution. However, carbon dioxide can be used as a source of high-value chemicals, as a source of sustainable energy. So far, many activities have been done to convert CO_2 into chemical materials, which can be applied as fuel for the industries.

With the increasing demand for energy and population growth, CO_2 emissions have grown as a by-product of power and industrial plants. In the last decade, CO_2 conversion has increased to other beneficial products. This process is useful for reducing pollution and warming of the earth. Developing a variety of electrocatalysts with high efficiency and good stability is a crucial issue [1].

The electrochemical CO_2 reaction reduction in recent decades has become crucial because it is a good reaction to artificial fuels and energy storage. When this process is linked to renewable energy sources such as solar cells, it can be a good alternative to fossil fuels. It also reduces CO_2 emissions in the atmosphere. But there are major problems for the reaction of CO_2 reduction, which includes low efficiency and low catalytic activity with cost-effective catalysts. Therefore, there is an important challenge in the present research, so that catalyst with better selectivity and higher activity and stability can be developed [2].

In recent years, several studies were done on various electrocatalysts, but yet, there are problems in Faradaic Efficiency (FE), Current Density (CD), Energy Efficiency, electrocatalyst deactivate, the internal resistance of electrocatalysts, and the potential for scalability to the large sizes without the loss of efficiency, because CO_2 is a thermodynamically stable molecule, it is fully oxidized [3–12]. A suitable electrocatalyst to reduce CO_2 is necessary to reach a low-cost process with acceptable selectivity and efficiency. In recent decades, the electrochemical reduction of CO_2 has interested a lot of consideration as low-cost electricity can come from renewable sources of energy such as solar and wind [13–18].

1.1 Zn-Ni coating

Zinc as another choice of cadmium has been studied for its ability to resist corrosion regarding its sacrificial properties and has demonstrated its ability to provide adequate corrosion behavior results through the study conducted on mechanical properties and corrosion protection of Zn electrodeposition [19]. Though Zn is considered a possible option, its corrosion behavior does not look acceptable in an aggressive condition with greater temperatures. Electrodeposited Zn coatings study tests indicated that pure Zn has weak corrosion resistance properties compared to cadmium [20]. Therefore, the need for metal coatings with corrosion properties outstanding to those of pure Zn and comparable or improved to cadmium has driven the industrial production of electrodeposits involving Zn alloys with VIIIB-group metals (e.g. Zn-Fe, Zn-Ni, Zn-Co) [21]. The electrodeposition of Zn and its eight-group metals including Co, Fe, and Ni have been extensively investigated and analyzed for their ability to be an excellent corrosion resistant alloy.

1.1.1 Zinc-nickel alloy corrosion behavior

In recent years, a lot of research has been performed to investigate the possibility that the Zn-Ni alloy could be a substitute with a corrosion property corresponding to the toxic coatings of cadmium. Much research has also been done to distinguish and determine the corrosion resistance of the Zn-Ni coatings [22–25]. The corrosion resistance of deposited Zn-Ni coatings on steel substrate indicated as having the acceptable corrosion property (corrosion rate: ~ 11 mm/year) was reached for Zn-Ni alloys in the range from 12 to 15 wt.% of Ni content in the coating so that the coating with Ni content from 12 to 15 wt.% maintains the anodic behavior of the steel, retaining the sacrificial behavior with a decrease corrosion rate after the addition of Ni, which increases the potential nearer to the substrate providing protection for a too time [21]. This has been endorsed by reports conducted by other authors [22–25] who have stated that Zn-Ni coating with a Ni amount of 12 to 15 wt.% supplies

adequate corrosion protection. While the coating retains its sacrificial behavior regarding the steel substrate, whenever the alloy with more than 30 wt.% of Ni turns nobler than the substrate, missing its sacrificial behavior. Hence, it led to preferential corrosion of the steel, and Ni amount of less than 10 wt.% in the coating produced smaller barrier performance. Byk et al. [25] performed tests showing the greatest corrosion resistance properties utilizing a poor acid chloride solution with the Zn-(15 wt.%) Ni coating having the least corrosion CD, demonstrating the best corrosion protection, and this is qualified to the existence of the γ phase (Ni_5Zn_{21}) which is gained with Zn-Ni coatings with Ni amount from 12 to 15 wt.% [25]. The coatings of Zn-Ni coating with 10–15 wt.% of Ni have more suitable corrosion resistance, better weldability, and superior formability. The presence of Ni in the Zn-Ni alloy in the optimal range from 12 to 15 wt.% reduces the rate of Zn dissolution, supplying greater and longer corrosion resistance than pure Zn [24].

1.2 CO₂ reduction reaction

Environments change due to greenhouse gases (CO_2) is a significant hazard to the protection of human society. The capture and conversion of carbon to the value-added chemical are attended to be the most agreeable method to prevent the rise of CO_2 in the environment as seen in **Figure 1**. But the cost of high technology accessible to capture, store, and convert CO_2 stops its functional operation [26]. Recycling CO_2 and transforming it into value-added chemicals create challenges for researchers in the area of catalysts. Among the various methods, the electrochemical method has unique advantages [27–29]. Most of the electrochemical reactions can be seen in small to industrial conditions. Besides, if the electricity is required from renewable sources, these sources of energy generate the required electricity, CO_2 will not be produced and, therefore, will have a good effect on the worldwide CO_2 level [30].

Studies showed that CO was an intermediator and also methane (CH_4) or ethylene (C_2H_4) was generated from HCO* or COH* intermediates. Norskov et al. presented details of reaction pathways to produce C_2H_4 and CH_4 from the CO_2 reduction reaction at copper catalysts using the Density Functional Theory (DFT) [31–34].
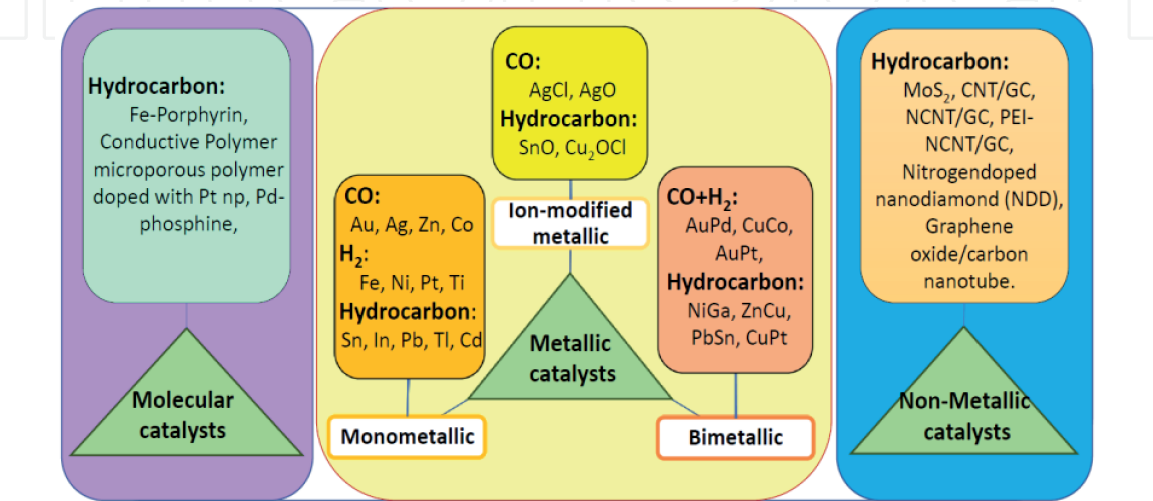

Figure 1.
Graphical schematic of the influence of CO₂ on the globe and conversion of CO₂ to the useable energy.

The outcomes demonstrated that the formation of HCO* was a key step for the reaction. They also compared the carbon dioxide reduction reaction in several transition-metal electrodes and determined that copper is the most efficient electrode for this case [35]. In the electrolysis of CO_2, the anode and cathode were located on separate sides, which were interconnected with a membrane in the middle of them. In the anode, the water oxidized to ion hydrogen (H^+) and molecular oxygen (O_2), while in the cathode, CO_2 was reduced to carbon compounds, and hydrogen was reduced [36]. The electrocatalysts for the reduction reaction of CO_2 totally divided into a few different classes as seen in **Figure 2**. Metals such as Ni, Pt, Al, Fe, Ti, and Ga were used as the catalysts for H_2 production, and CO was not created as the main product [50–53]. The H_2 evolution reaction rates by these group metals are commonly greater than that of the CO_2RR rate.

Another class of metals of Ag, Au, and Zn convert CO_2 to CO with an acceptable efficiency [54]. Catalysts consist of In, Pb, Hg, and Sn convert CO_2 to formate as the main product. On these metals, the mechanism of CO_2RR to formate is different in which there is no breaking of the C-O bond. Electrodes including W, Cr, and Mo have been reported as inadequate catalysts because of weak selectivity and reduction rate. Copper as a metal catalyst can react to a reduction in CO_2 to alcohol and hydrocarbons (C_2H_4, CH_4, CH_3OH). However, recent research had shown that the CO_2RR to these fuels was made at lower efficiency, which was influenced by the binding-energy of the intermediate species of CO. For example, Ag and Au catalysts can produce CO more rather due to less energy for intermediate carbon monoxide molecules. Since it can be evolved from the surface without more reaction. Therefore, producing higher carbon species at these levels is extremely minimal. However, Cu is a unique catalyst that allows it to produce various carbonaceous products (such as, alcohol and hydrocarbons) with higher activity [54].

Electrodes play a key role in all reactions according to heterogeneous electrochemical reactions, such as CO_2RR [55]. The durability and performance of the electrochemical cells are essentially defined by the processes happening at the electrolyte-electrode interface. Overall, electrodes include an electrocatalyst layer as well as a backing layer or substrate that attend multiple acts: firstly, to transport reactant gases, CO_2, from the electrolyte to the catalyst layer; secondly, to derive products from the catalyst layer into the membrane/electrolyte; and lastly, electrons connectivity with little resistance [55–58]. Most electrode efficiency, and accordingly electrochemical cell efficiency, requires enhancing all these three processes that greatly relate to the complicated microstructure of the electrodes. Till now, the

Figure 2.
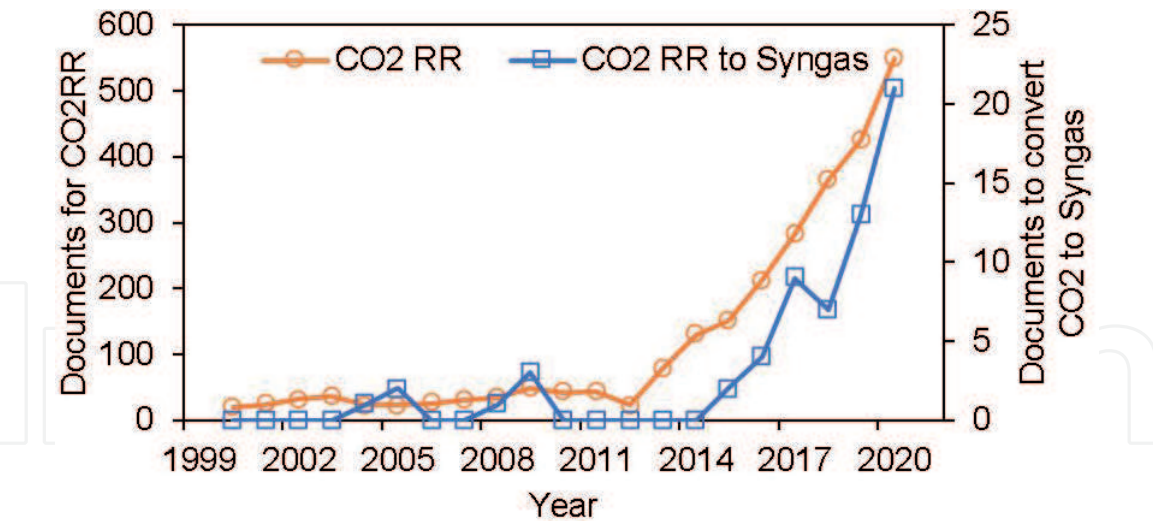*A set of three main categories of electrocatalysts for CO_2 reduction reaction [36, 37–49].*

nanoparticles of Ag [59, 60], Sn [61], Au [62], MoO_2 [63, 64], Bi [65], MoS_2 [62], etc., coated on low carbon steel substrate and $Cu_2O/TiO_2/FTO$ [66] have been utilized to convert CO_2 to CO applying room-temperature ionic liquids (RTILs) as electrocatalysts. Nevertheless, none of these materials enabled the development of CO with a CD of >100 mA/cm^2 in CO_2RR during controlled potential electrolysis (CPE) tests in combination with any of the utilized RTIL assistant catalysts, which is required to commercially use any of these procedures. In the last decade, the electrochemical CO_2RR had been widely considered [67–69]. The reduction reaction products of electrochemical CO_2RR on the Cu-based electrodes are hydrocarbons for example C_2H_4 and CH_4 [70–72]. Practical investigations on the electrochemical CO_2RR in the base electrodes of copper showed that the exhaust gas contains CO, CH_4, C_2H_4, and primary alcohol that depended on their electrolyte [73, 74]. There were numerous studies of electrochemically CO_2 reduction reaction on Cu-based electrodes [37–39].

Table 1 shows the summarized characterization of electrocatalysts for the CO_2RR to various. As shown in **Table 1** and **Figure 3** for SYNGAS (CO + H_2) production,

Electrocatalysts	Faradaic Efficiency	Current Density (mA/cm^2)	Main product	Ref.
Fe-Porphyrin	—	< 5	**Hydrocarbon**	[75]
Sn-based	91%	15		[61]
nano-SnO$_2$	80%	9		[76]
Sn foil	<20%	< 5		[76]
Sn/SnO$_x$ nanoclusters	<40%	—		[76]
Ni-Ga	<70%	<1		[77]
Molybdenum disulphide	~90%	65		[62]
Cl-induced bi-phasic Cu2O–Cu	~70%	<0.2		[76]
Conductive Polymer microporous polymer doped with Pt np	>95%	—		[78]
Strontium-doped lanthanum	<15%	<20		[79]
Iridium/Ruthenium Oxide	~90%			[80]
Zn-Cu	60%	4		[49]
Pb - Sn	—	2.5		[35]
Zn-Co based	70%-	8		[3]
Cu-Pt	<38%	—		[81]
Cu-Ni	<40%	—		[82]
Ni-based	80%	5		[3]
CNT/GC	<10%	~2		[76]
NCNT/GC	60%	~4		[76]
PEI-NCNT/GC	<85%	~10		[76]
Nitrogendoped nanodiamond	90%	~1		[76]
Pd –based	<50%	<5	(CO + H_2) Syngas	[83]
Au$_{0.76}$ –Pd$_{0.24}$	~90%	<10		[84]
Cu-Co	33%	8		[85]
Au$_{0.78}$ –Pt$_{0.22}$	~90%	0.6		[86]
Cu-Ag	~64%	10		[87]

Electrocatalysts	Faradaic Efficiency	Current Density (mA/cm^2)	Main product	Ref.
Bismuth- based	<90%	<4	**Carbon monoxide (CO)**	[65]
[EMIM]BF$_4$-Bi	93%	4		[76]
Graphene oxide/carbon nanotube	85%	2.3		[88]
carbon paper	68%	0.9		[89]
Sn/SnO$_x$ nanoclusters	<60%	—		[76]
Zn electrode	64%	2.8		[76]
Zn porous	77.9%	8		[76]
Zn dendrite	80%	12		[49]
Zn hexagonal	~83%	4.4		[75]
Cu polycrystalline	30%	—		[76]
Au np	>90%	81		[43]
Au bulk	80%	2.2		[45]
Oxide Derived-Au	—	10		[40]
Ag bulk	82%	2.0		[59]
Ag np	~80%	29		[44]
Ag np	92%	10		[46]

Table 1.
Product distribution for electrochemical CO$_2$ reduction reaction on various electrocatalysts.

Figure 3.
Total published documents for the electrochemical CO$_2$ reduction reaction and specifically convert CO$_2$ to SYNGAS in terms of over time [Scopus data based].

there is not enough research in this field. Also, for the production of SYNGAS, the Au$_{0.76}$–Pd$_{0.24}$ electrocatalyst has the highest Faraday efficiency (~90%) and CD (~10 mA/cm^2), which is a high-cost and unsuitable alloy electrode for large-scale use [42]. Other electrocatalysts for SYNGAS production have low FE and/or low CD, as can be seen in **Table 1**. The Ag/Au nanostructure catalysts for electrochemical CO$_2$RR to CO with a FE of further than 90% and a CD greater than 30 mAcm^{-2} have been stated by researchers [40–43]. Zinc performs as an electrocatalyst for CO$_2$RR to CO, while it is a cost-effective, non-noble, and abundant choice to gold and silver [44].

There are also statements of nano-structured Zn catalysts including hexagonal, dendritic, and nanoscale [45–47]. Quan et al. have reported Zn nanoscale and Zn foil as a catalyst for the CO_2RR at the NaCl and $NaHCO_3$ electrolytes. They demonstrated that the nano-scale catalyst at NaCl cathodic solution has the greatest proficiency in terms of CD and FE about 6 $mA.cm^{-2}$ and > 90%, respectively, at a potential of −1.6 V by linear sweep voltammetry (LSV) method [45]. Rosen et al. have studied Zn balks and Zn dendrite catalysts for the electrochemical CO_2RR in 0.5 M $NaHCO_3$ cathodic solution. They stated Zn dendrite electrocatalyst has a CD of 4 $mA.cm^{-2}$ at the potential value of −1.14 V (*vs.* RHE) and FE of 80% [46]. By modifying the surface microstructure, morphology, or orientation of the Zn catalyst, the more FE and product selectivity can be attained for converting CO_2 to CO.

Nguyen et al. showed that microstructural or morphological changes in catalysts play a significant role in developing CO_2RR [48]. The surface of the Zn catalyst is simply oxidized although immersed in aqueous solutions or exposed to air. Thus, situations should be restricted to avoid zinc oxidation [48]. Nguyen et al. have also reported a porous nanostructure of the Zn catalysts which were prepared of zinc-oxide for the CO_2RR. By applying this porous metal, they obtained a faradaic efficiency of 78.5% for CO_2RR at a potential value of −0.95 V (*vs* RHE) in the $KHCO_3$ electrolyte [48]. Keerthiga and Chetty have reported a modified zinc-copper catalyst for the CO_2RR to hydrogen, C_2H_6, and CH_4 products. They coated zinc on the copper with different concentrations of electrolytes, and the outcomes were evaluated with pure Cu and Zn catalysts. They showed that zinc-copper with a high-level concentration of electrolyte had superior performance, also, the FE of CH_4 was the order Zn (7%) < Cu (23%) < Cu-Zn (52%). Moreover, the H_2 FE for Cu and Cu-Zn were 68% and 8%, respectively [49].

In this way, it has been selected inexpensive materials as electrocatalysts for commercial and industrial applications. Electrocatalysts must be appropriate that could have acceptable efficiency and cheap price for the reforming process. By referring to **Figure 2**, zinc and nickel are affordable materials for carbon monoxide and hydrogen production, respectively. Hence, to produce SYNGAS (CO + H_2) in this study, the Zn-Ni bimetallic material is chosen from these two groups of catalysts for CO and H_2 products. Other electrocatalysts are either inefficient or expensive. This work aims to investigate the Zn_x-Ni_{1-x} coatings for the electrochemical CO_2 reduction reaction.

2. Experimental methods

2.1 Preparation and investigation of Zn-Ni Electrocatalyst for CO_2 reduction reaction

Zinc-nickel Alloys were coated on the low-carbon steel substrate by chronopotentiometry method at different electrochemical parameters. Then, Zn-Ni coatings were investigated in terms of microstructure, microcrack formation, and coating composition using SEM / EDX analysis and corrosion resistance by Autolab potentiostat (Model: PGSTAT128N) to obtain the coating with the best performance and quality. Besides, the coatings were analyzed using SEM/EDX analysis after CO_2 reduction reaction for microstructure and coke formation, as well as gas efficiency by gas chromatography analyzer. Nickel chloride hexahydrate ($NiCl_2.6H_2O$), ammonium chloride (NH4Cl), and zinc chloride ($ZnCl_2$) of raw materials were utilized for bath electrolyte preparation and ammonia solution (25%) for pH modification. All electrolytes were made using distilled water. The zinc and nickel alloy solutions were prepared in the laboratory to allow the study of the deposition at different bath solution temperatures. The pH of the solution was measured using a pH meter.
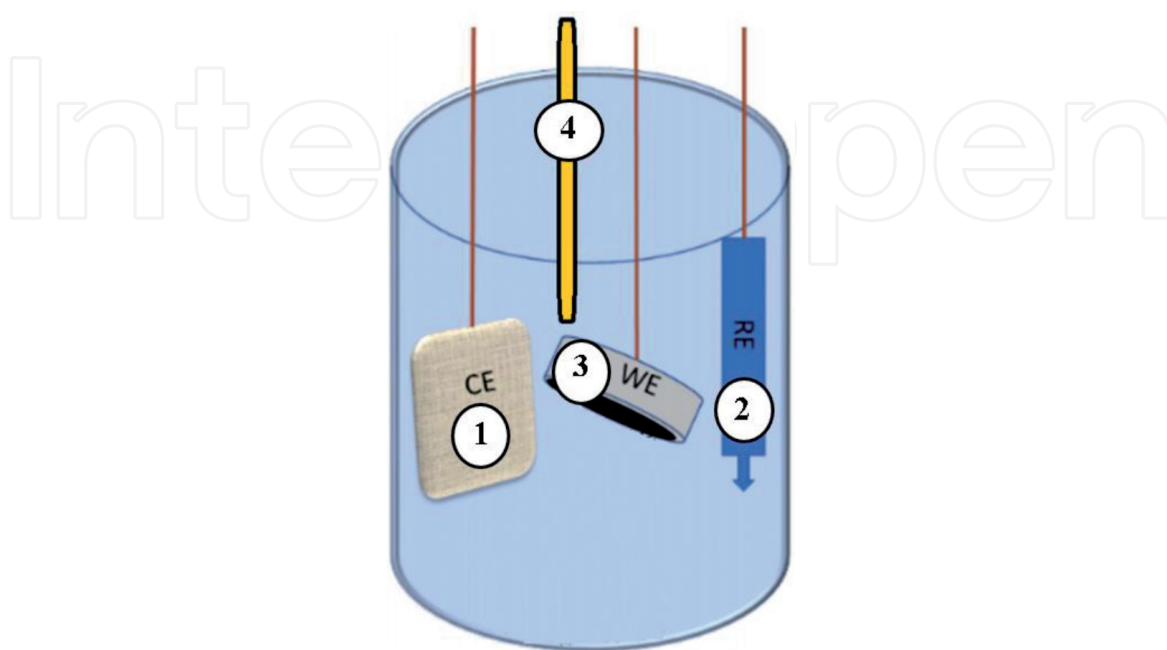
Ammonia solution (25%) was used to raise the pH of the electrolyte to the needed level of pH 5. The solution was stirred using a glass rod and the pH measuring was taken applying a pH meter, continuously. Chronopotentiometry electrodeposition was applied at different bath solution temperatures of 25°C, 40°C, 60°C, and 70°C. There were three types of electrodes, low carbon steel (working electrode), Ag/AgCl (reference electrode), and Pt mesh (counter electrode). The electrodeposition process was performed galvanostatically for each deposition temperature. The experimental setup for electrodeposition was performed as seen in **Figure 4**.
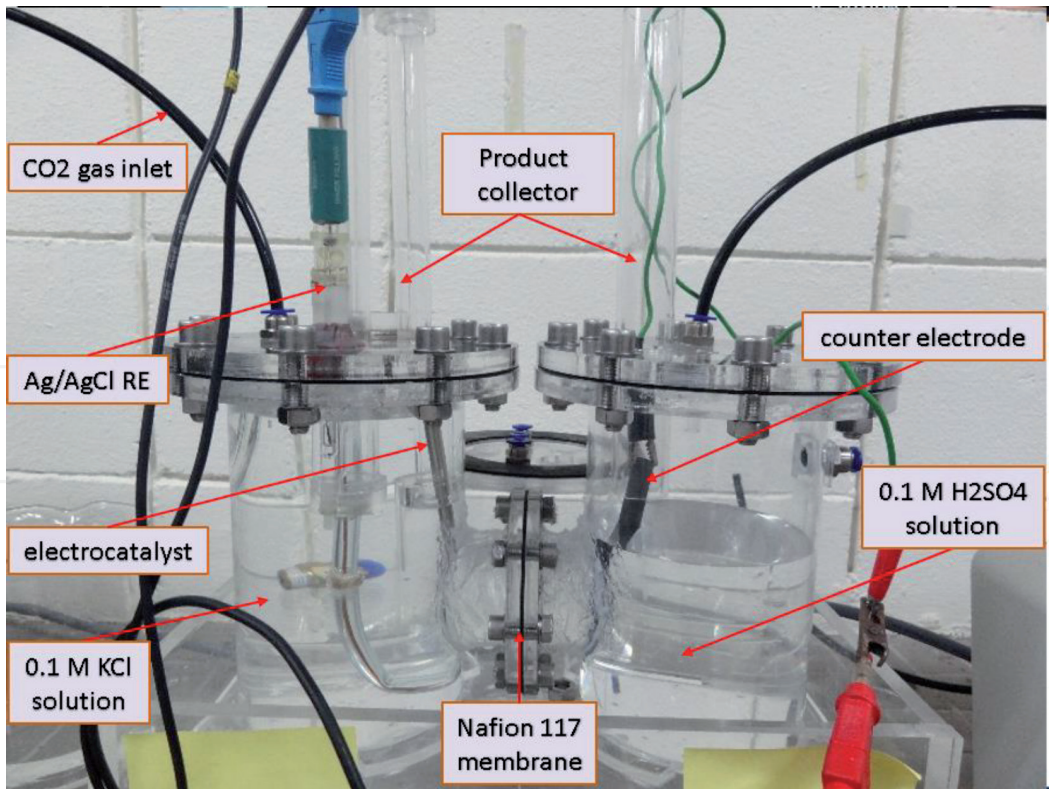
The deposited Zn-Ni coatings were analyzed on their compositional and microstructural properties applying SEM. The morphologies were observed and investigated for the electrodeposited zinc-nickel alloy samples at different temperatures of the bath solution. The material composition is determined by the SEM equipped with EDX which shows the composition information of the alloy coating. Linear polarization resistance (LPR) analysis was performed regarding the ASTM standard of G 96.– 90 (Reapproved 2001)e1.

2.2 Electrochemical CO_2 reduction reaction

For CO_2RR an H-shaped electrochemical cell was used which has 2-chambers (cathodic and anodic sections) that were connected with membrane Nafion 117 as seen in **Figure 5**. CO_2 gas was inserted into the cathodic section for the reduction process. In this method, electrocatalyst, reference electrodes (Ag/AgCl), and CO_2 saturated cathodic electrolyte were in the cathodic part, where CO_2RR happened, in the other part, the counter electrode (graphite) and anodic electrolyte (0.1 M H_2SO_4) were placed where the oxidation occurred. It was, therefore, predicted that SYNGAS (H_2 + CO) and coke would form in the cathodic portion, and O_2 would be produced in the anodic portion. Working, reference, and counter electrodes (WE, RE, and CE), were linked to the Autolab potentiostat device (Model: PGSTAT128N) to inspect potential and current records. A gas bag was attached to the exhaust to collect products for gas chromatography to characterize gases. Images of the catalyst morphologies were examined utilizing SEM. The catalysts were analyzed by EDX for coke formation and electrocatalyst surface compositions.

Figure 4.
Electrodeposition setup for Zn-Ni coatings, (1) counter electrode, (2) reference electrode (3) working electrode, (4) thermometer.
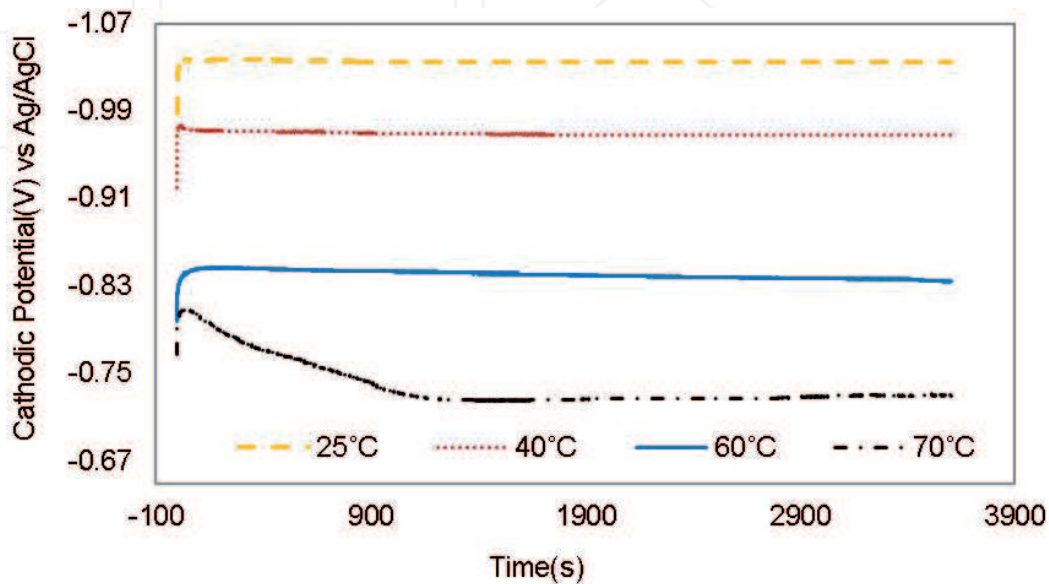
Figure 5.
Cell setup for electrochemical CO_2RR by Zn-Ni electrocatalyst, graphite CE, 0.1 M KCl (cathodic solution), H_2SO_4 (anodic solution) and Ag/AgCl RE.

3. Results and discussions

3.1 Zn-Ni electrodeposition

The cathodic protection (CP) graph at various temperatures for the Zn-Ni deposition is displayed in **Figure 6**. The graph of the potential in terms of time for Zn-Ni coating depositions at 25°C, 40°C, 60°C, and 70°C were seen throughout
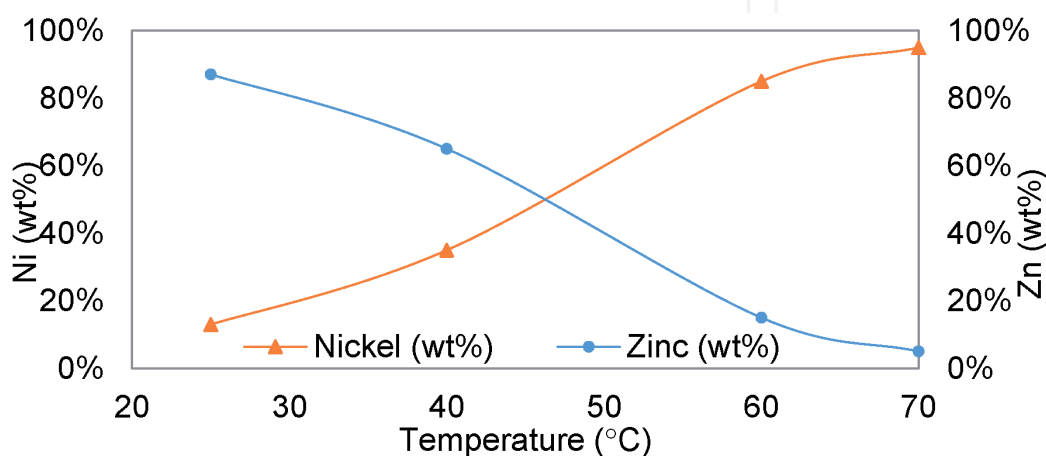

Figure 6.
Deposition potential of Zn-Ni coatings in terms of time by chronopotentiometry method at various bath solution temperatures.

the electrodeposition process. A decrease (more positive) in CP was detected over time with increasing temperature. The CP in chronopotentiometry was related to the ion's concentration becoming reduced at the substrate surface in response to the utilized current.

The standard potential E_o (V) for Ni and Zn is $-0.25V$ and 0.76 V (vs. SHE), respectively [90]. The CPs seen in the deposition were nearest to E_o (V) of the reactants that were converted to its metal. Therefore, the outcomes on the decrease in CP towards a further positive amount over time for electrodepositions at high temperature (60°C and 70°C) demonstrated the CP's deposition was shifting nearer to E_o (V) of Ni reduction, favoring the reaction of Ni-ion reduction to Ni-solid on the substrate. This opinion was more confirmed by EDX outcomes (**Figure** 7). The rise in Ni amount was assigned to a decrease in CP (more positive) over time through the electrodeposition reaction. This supposition is reported by Velichenko et al. [91], who stated the decrease in CP with rising Ni-ion concentration in the bath solution resulting in an improvement in Ni deposition. Qiao et al. [92] detected similar findings of reducing CP with increasing deposited Ni amount in the surface deposition with rising temperature.
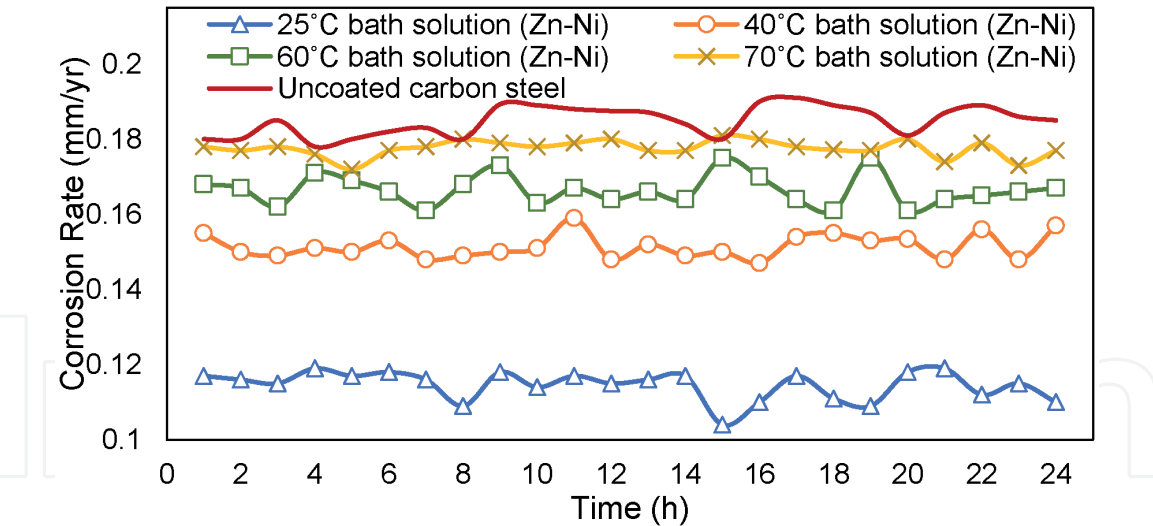
3.2 Linear polarization resistance testing for Zn-Ni deposits

Zn and Ni amounts in the coatings have a considerable effect on the corrosion properties of Zn-Ni deposits. As revealed by Baldwin et al. [93] and Conde et al. [21], the lowest corrosion rate is obtained when the Ni amount is between 12 wt.% to 15 wt.% in the coating. Zn being a lower noble metal plays as an anode that sacrifices in relative to the substrate under a standard situation. Zn is extra favored compared with a nobler metal for instance Ni to be developed into coatings regarding its further sacrificial behavior. But adding more noble elements to Zn improves the corrosion resistance of Zn. By adding Ni to Zn, the rate of sacrificing of coating for the substrate is lower compared to bare Zn. Ni act to hinder or reduce the dissolution rate of Zn. But, when the Ni amount in the coating enhancements to more than 30%, the sacrificial performance decreases, and the coating turn nobler compared to the substrate (Steel). At this stage, the corrosion rate is entirely according to the coating characteristics. As seen in **Figure 8**, with rising temperatures, the corrosion rate increases. This shows that adding Ni to Zn no more enhances corrosion resistance. The coating turns nobler than the substrate and the existence of cracks that are detected causing a rise in the corrosion rate. As the bath solution temperature increases, hydrogen reduction occurs around the working electrode,

Figure 7.
EDX analysis results in terms of Zn and Ni contents (wt%) vs. bath solution temperature (°C).
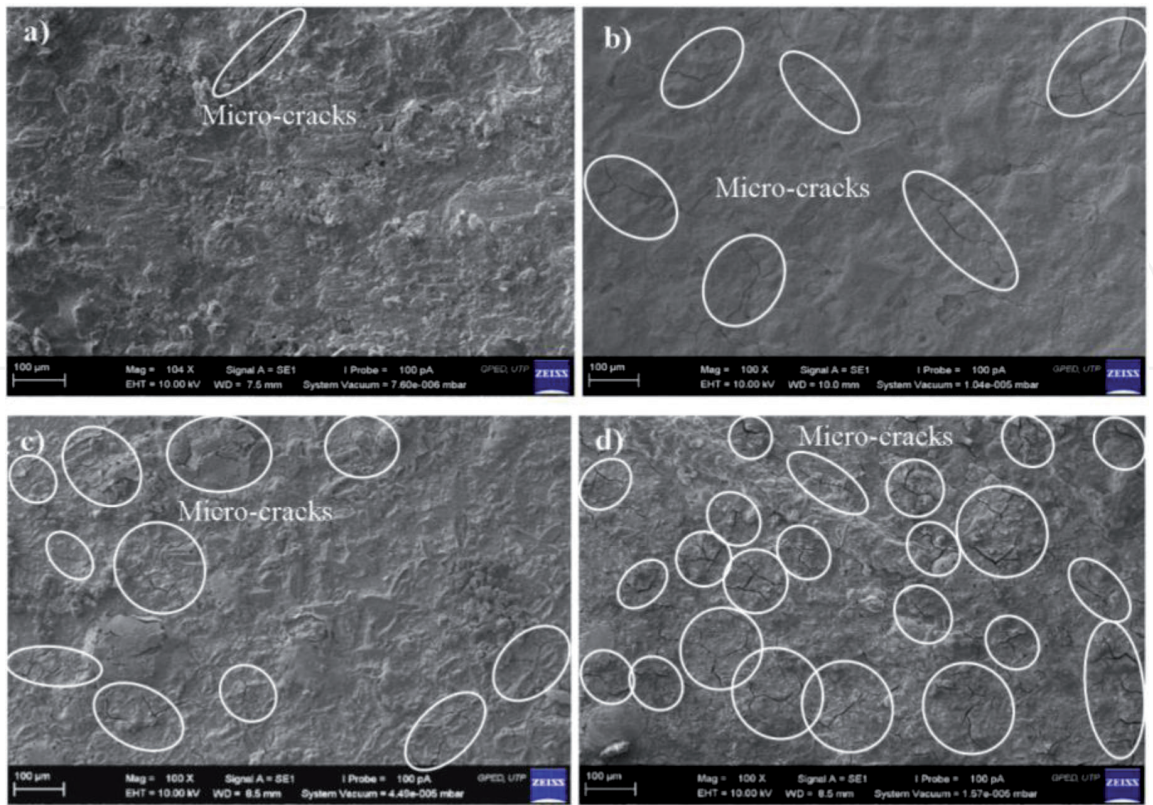
Figure 8.
LPR corrosion rate measurements taken for Zn-Ni alloy coatings vs. uncoated carbon steel for hourly for 24 h.

which creates bubbles form on the surface that prevents the deposition. On the other hand, hydrogen penetrates the coating and makes internal stress. The cracks and disruptions (as shown in **Figure 9**) in the coatings increase speed the corrosion rate of the substrate. These clarify the important variation in the corrosion rate for coatings deposited at 25°C and 40°C, 60°C, and 70°C.

The ratio of Zn and Ni for deposits formed at 25° C is in the optimal range of Ni amount from 12 to 15 wt.%. Therefore, the sacrificial performance of Zn is retained relative to the adding of the Ni, and this makes the steel substrate with decreasing corrosion rate as Zn acts as an anode. By adding 12–15 wt.% of Ni, the dissolution rate of Zn slows down, and the corrosion rate reduces. The cracks and defects in the

Figure 9.
SEM images for electrodeposition of Zn-Ni alloy coatings at temperature of (a) 25°C, (b) 40°C, (c) 60°C, and (d) 70°C of bath solution.

deposits do not substantially influence the corrosion properties of the metal layers, as further anodic Zn causes preferential corrosion.
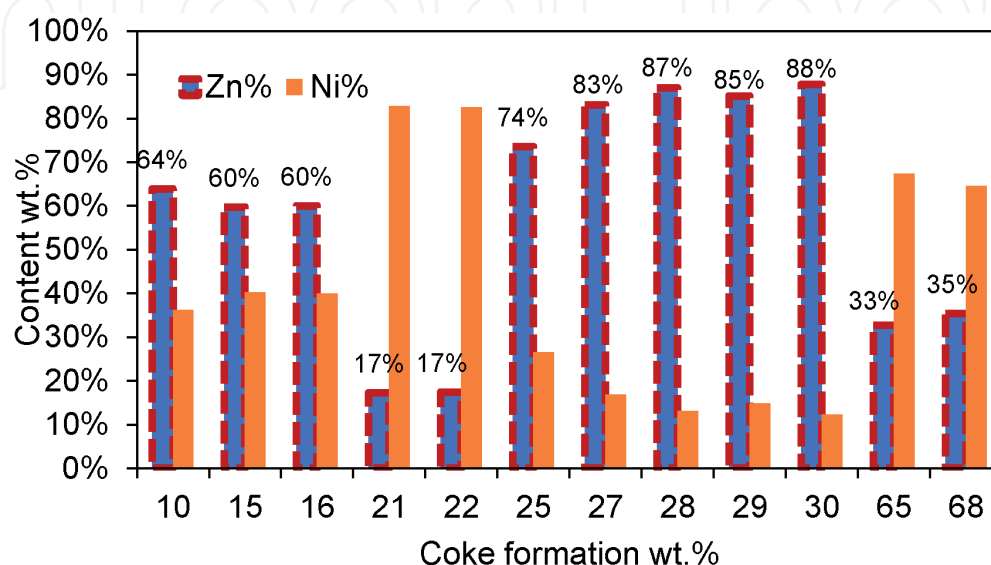
3.3 SEM and EDX analysis for Zn-Ni deposits

As the bath electrolyte temperature raises, the ion mobility in the electrolyte rises. Hence, the coatings can be smoother. However, the SEM results displayed in **Figure 9** indicate that microcracks are detected in all deposited coatings at various temperatures. The micro-cracks intensity with rising the bath solution temperature is considered to be 25°C < 40°C < 60°C < 70°C. The microcracks formation can depend on the internal stress created and the evolution of hydrogen during the deposition. As the temperature increased, the evolution of hydrogen happened.
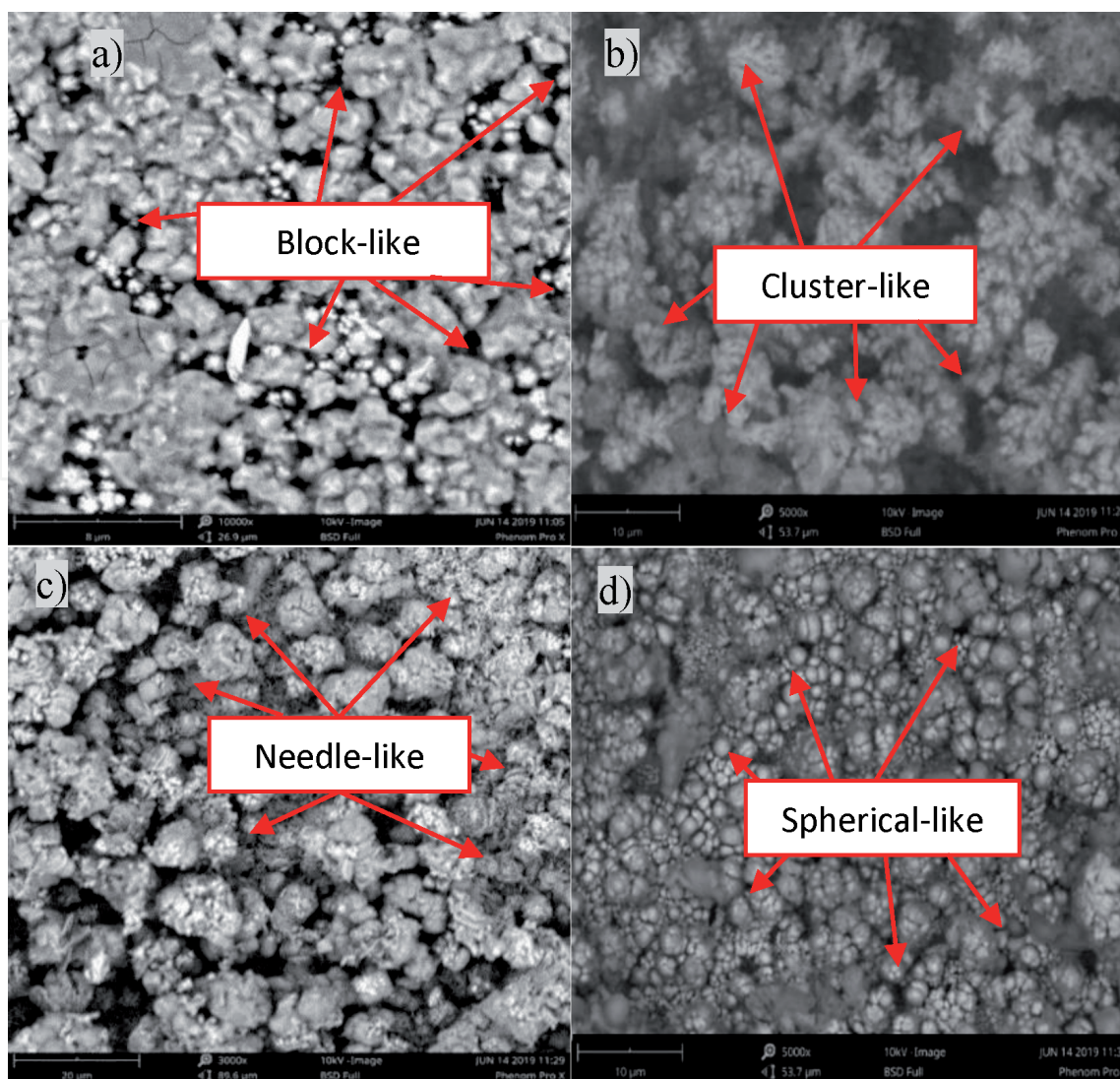
Enhancement of inner stress through deposition can be attributed to a lot of reasons. Alfantazi et al. [94] revealed the existence of microcracks in Zn-Ni coatings when the Ni amount in the coating increased. Qiao et al. [92] and Rehim et al. [95] reported the micro-cracks in the Zn-Ni coatings deposited in the acidic bath solution were attributed to H_2 embrittlement via the H_2 evolution. A rise in the hydrogen release was observed with the outputs of a rise in the hydrogen CD with the temperature rises. This H_2 reduction reaction causes H_2 atoms to penetrate the coated layer, straining the crystal lattice, and causing high-stress internal cracks.

3.4 Investigation of Zn-Ni bimetallic electrocatalysts for CO_2RR

To realize the impacts of the catalysts for the CO_2RR, the composition, morphology, and structure of the catalysts were investigated. **Figure 10** and **Figure 11** display EDX results and SEM images of the Zn-Ni with various compositions after the 48 h for the CO_2RR by cyclic voltammetry with scan rate 0.05 V. s^{-1}, graphite counter electrode, 0.1 M KCl cathodic, and 0.1 M H_2SO_4 anodic solutions. According to EDX analysis, as shown in **Figure 10**, carbon with ~28–30 wt.% was deposited on the $Zn_{85\%}$-$Ni_{15\%}$ electrocatalyst after 48 h of testing. The microstructure of $Zn_{0.85}$ - $Ni_{0.15}$ is a block-like morphology in which carbon is almost uniformly distributed in the substrate due to CO_2 reduction. As can be seen in **Figure 11(a)**, some electrocatalytic regions are carbon-covered, preventing CO_2 reduction over time. Therefore, for further consideration of this electrocatalyst, gas chromatography of produced gases (the produced gases were collected with the gas bag) has been investigated.
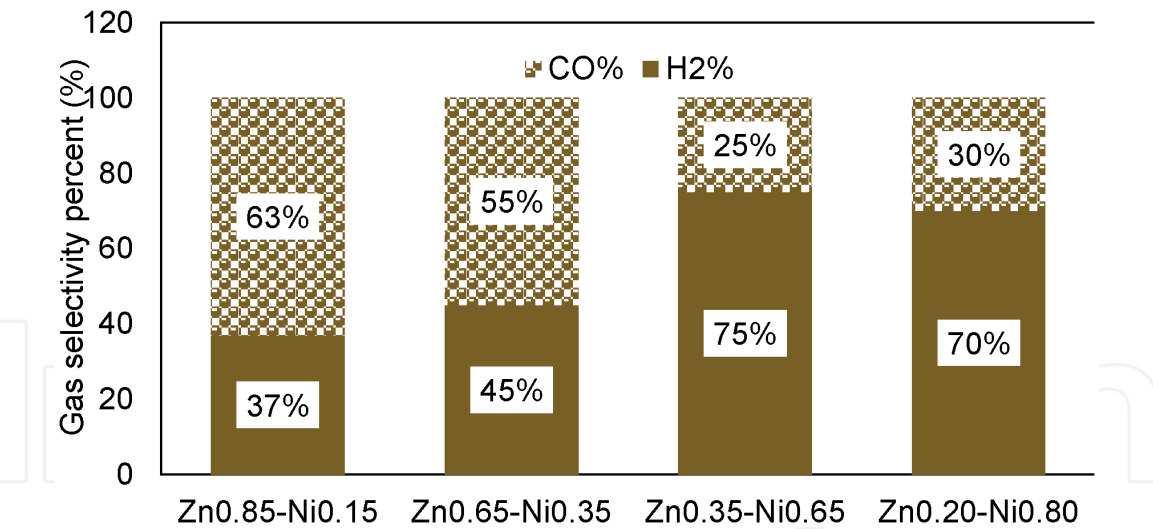

Figure 10.
EDX results of C content (wt.%) in terms of Zn-Ni compositions after 48 h of electrochemical CO_2RR.

Figure 11.
SEM images of Zn-Ni electrocatalysts after 48 h of CO_2RR on (a) $Zn_{85\%}$-$Ni_{15\%}$, (b) $Zn_{65\%}$-$Ni_{35\%}$, (c) $Zn_{35\%}$-$Ni_{65\%}$, and (d) $Zn_{20\%}$-$Ni_{80\%}$ electrocatalysts.

According to EDX analysis, as shown in **Figure 10**, carbon with ~10 wt.% was deposited on the $Zn_{65\%}$-$Ni_{35\%}$ electrocatalysts after 48 h of testing. As shown in **Figure 11(b)**, the microstructure of the $Zn_{65\%}$-$Ni_{35\%}$ electrocatalyst is a cluster-like morphology where coke formation is minimized by the reaction of CO_2 with this microstructure after 48 h. With comparing Zn_x-Ni_{1-x} electrocatalysts, with decreasing Zn amount in Zn_x-Ni_{1-x} coatings from 85 wt.% to 65 wt.% of Zn, coke formation upon Zn-Ni electrocatalysts decreases. Furthermore, the electrocatalyst microstructures have changed from block-like to cluster-like with decreasing Zn content from 85 wt.% to 65 wt.%. Therefore, the activity and efficiency of electrocatalysts increase with decreasing Zn content from 85 wt.% to 65 wt.% in Zn-Ni electrocatalysts. By further reducing the amount of Zn until ~33 wt.%, coke formation upon Zn-Ni electrocatalyst increases.

Furthermore, as seen in **Figure 11c**, the microstructure of the $Zn_{35\%}$-$Ni_{65\%}$ electrocatalyst is semi-spherical, where carbon was deposited between the semi-spherical grains with needle-like microstructure. This high coke formation is due to changes in the microstructure and electrocatalytic activity due to the interaction between Zn and Ni with the ions present in the solution. By further reducing the amount of Zn up to 20 wt.% in the Zn-Ni coating, the coke formation (after 48 h of CO_2RR) on the electrocatalyst decreased. The microstructure of 20%Zn-80%Ni is a glossy spherical morphology where carbon is grown with a dark semi-spherical morphology about 22 wt.%.

Figure 12.
Gas chromatography results for CO_2RR by various electrocatalysts in terms of CO and H_2 gas selectivity by cyclic voltammetry method.

Coating composition					Coating performance			
	Zn content (%)	Ni content (%)	CR (mm/yr)	Morphology		CO (%)	H_2 (%)	C (%)	Efficiency after 48 h (%)
				Coating	carbon				
Zn_x-Ni_{1-x}	85	15	0.11	Block-white	Block-black	63	37	30	53.33
	65	35	**0.15**	**Cluster-like**	**Low amount**	55	45	**10**	**66.00**
	35	65	0.17	Semi-spherical	Needle-like	25	75	65	31.88
	20	80	0.25	White Spherical	black Spherical	30	70	22	57.27

Table 2.
Zn-Ni Electrocatalysts performance with different compositions and electrodeposition parameters for CO_2RR.

Due to the results of gas chromatography, as shown in **Figure 12**, the $Zn_{85\%}$-$Ni_{15\%}$, $Zn_{65\%}$-$Ni_{35\%}$, $Zn_{35\%}$-$Ni_{65\%}$, and $Zn_{20\%}$-$Ni_{80\%}$ electrocatalysts have 63%, 55%, 25%, and 30% selectivity for CO and 37%, 45%, 75%, and 70% selectivity for H_2 products, respectively. Also, according to **Table 2**, the total efficiency for CO_2RR after 48 h of testing is 53%, 66%, 31%, and 57%, respectively. The $Zn_{65\%}$-$Ni_{35\%}$ electrocatalyst is appropriate in terms of morphology, stability, coke formation, product selectivity, and intensity of the electrochemical CO_2RR. The coke formation on the catalysts can influence the activity spots of the catalyst and have a negative impact on the efficiency and life cycle of the catalyst. Consequently, the chemical compositions, microstructure, and morphology of catalysts have a crucial role for the CO_2RR to produce gases with satisfactory ratio, desired product, least-coke formation, and suitable efficiency, activity, and stability.

4. Conclusions

The lower corrosion rate of coatings deposited at 25°C is mainly related to the role of nickel in zinc-nickel alloy and a higher corrosion rate at higher temperatures

of 40°C, 60°C, and 70°C are related to the lower barrier properties such as uniformity, compactness and cracks in the alloy. Zinc-nickel alloy coatings with the highest corrosion resistance, within required composition of 12–15%, dense and compact morphology, better uniformity with less crack is achieved with coatings deposited at 25°C. CO_2RR on Zn_x-Ni_{1-x} electrocatalysts in 0.1 M KCl as the cathodic solution and 0.1 M H_2SO_4 as the anodic solution using cyclic voltammetry method demonstrated that the $Zn_{65\%}$-$Ni_{35\%}$ electrode had the best performance for the CO_2RR with regarding the minimum coke formation (<10%) and optimal faradaic efficiencies of CO and H_2 (FE_{CO} = 55% and FE_{H2} = 45%). The coke formation on the catalysts can influence the activity spots of the catalyst and have a negative impact on the efficiency and life cycle of the catalyst. Consequently, the chemical compositions, microstructure, and morphology of catalysts have a crucial role for the CO_2RR to produce gases with satisfactory ratio, desired product, least-coke formation, and suitable efficiency, activity, and stability. Therefore, the $Zn_{65\%}$-$Ni_{35\%}$ electrocatalyst with cluster microstructure had the best performance for CO_2RR among other electrocatalysts in this study.

Author details

Mohammadali Beheshti*, Saeid Kakooei, Mokhtar Che Ismail
and Shohreh Shahrestani
Universiti Teknologi PETRONAS, Seri Iskandar, Malaysia

*Address all correspondence to: mohammadali_g03438@utp.edu.my

IntechOpen

References

[1] Yua F, Weia P, Yanga Y, Chena Y, Guob L, Peng Z. Material design at nano and atomicscale for electrocatalytic CO_2 reduction. Nano material. Science. 2019;1:60-69.

[2] Kortlever R, Balemans C, Kwon Y, Koper MTM. Electrochemical CO_2 reduction to formic acid on a Pd-based formicacid oxidation catalyst. Catalyst Today. 2015;244:58-62.

[3] Liu Y, Tian D, Biswas AN, Xie Z, Hwang S, Lee JH, Meng H, Chen JG. Transition Metal Nitrides as Promising Catalyst Supports for Tuning CO/H_2 Syngas Production from Electrochemical CO_2 Reduction. Angewandte Chemie. 2020;131. DOI: https://doi.org/10.1002/ange.202003625

[4] Derrick J, Loipersberger M, Iovan D, Smith PT, Chakarawet K, Long JR, Head-Gordon M, Chang C. Metal–Ligand Exchange Coupling Promotes Iron-Catalyzed Electrochemical CO_2 Reduction at Low Overpotentials. ChemRxiv. 2020. DOI: https://doi.org/10.26434/chemrxiv.11923176.v1

[5] Beheshti M, Kakooei S, Ismail MC, Shahrestani S. Investigation of CO_2 electrochemical reduction to Syngas on Zn/Ni-based electrocatalysts using the cyclic voltammetry method. Electrochimica Acta. 2020;341:135976. DOI: https://doi.org/10.1016/j.electacta.2020.135976

[6] Ma Z, Tsounis C, Kumar PV, Han Z, Wong RJ, Toe CY, Zhou S, Bedford NM, Thomsen L, Ng YH, Amal R. Enhanced Electrochemical CO_2 Reduction of Cu@Cux O Nanoparticles Decorated on 3D Vertical Graphene with Intrinsic sp^3-type Defect. Advanced Functional Materials. 2020: 1910118. DOI: https://doi.org/10.1002/adfm.201910118.

[7] Choi W, Won DH, Hwang YJ. Catalyst design strategies for stable electrochemical CO_2 reduction reaction. Journal of Materials Chemistry A. 2020;120. https://doi.org/10.1039/D0TA02633F

[8] Perry SC, Leung P, Wang L, Ponce de León C. Developments on carbon dioxide reduction: Their promise, achievements, and challenges. Current Opinion in Electrochemistry. 2020;20:88-98,2020. DOI:https://doi.org/10.1016/j.coelec.2020.04.014

[9] Zhao Y, Chang X, Malkani AS, Yang X, Thompson L, Jiao F, Xu B. Speciation of Cu Surfaces During the Electrochemical CO Reduction Reaction. Journal of the American Chemical Society. 2020;142(21):9735-9743. DOI:https://doi.org/10.1021/jacs.0c02354

[10] Zhang L, Merino-Garcia I, Albo J, Sánchez-Sánchez CM. Electrochemical CO_2 reduction reaction on cost-effective oxide-derived copper and transition metal–nitrogen–carbon catalysts. Current Opinion in Electrochemistry. 2020;23:65-73.

[11] Zhang T, Han X, Yang H, Han A, Hu E, Li Y, Yang X, Wang L, Liu J, Liu B. Atomically Dispersed Nickel(I) on an Alloy-Encapsulated Nitrogen-Doped Carbon Nanotube Array for High-Performance Electrochemical CO_2 Reduction Reaction. Chemistry Europe. 2020. DOI: https://doi.org/10.1002/ange.202002984

[12] Garg S., Li M., Rufford TE, Ge L, Rudolph V, Knibbe R, Konarova M, Wang GGX. Catalyst–Electrolyte Interactions in Aqueous Reline Solutions for Highly Selective Electrochemical CO_2 Reduction. 2020. DOI: https://doi.org/10.1002/cssc.201902433

[13] Popović S, Smiljanić M, Jovanovič P, Vavra J, Buonsanti R, Hodnik N. Stability and Degradation Mechanisms of Copper-Based Catalysts for

Electrochemical CO_2 Reduction. chemical Society. 2020. DOI:https://doi.org/10.1002/anie.202000617

[14] Gunathunge CM, Li J, Li X, Hong JJ, Waegele MM. Revealing the Predominant Surface Facets of Rough Cu Electrodes under Electrochemical Conditions. ACS Catalysis. 2020;10(12):6908-6923. DOI:https://doi.org/10.1021/acscatal.9b05532

[15] Yu H, Jiang J., Accelerating catalysts design by machine learning. Science Bulletin. 2020. DOI: https://doi.org/10.1016/j.scib.2020.06.004

[16] Zhi X, Jiao Y, Zheng Y, Vasileff A, Qiao SZ. Selectivity roadmap for electrochemical CO_2 reduction on copper-based alloy catalysts. Nano Energy. 2020;7(1):104601.

[17] Rutkowska IA, Wadas A, Szaniawska E, Chmielnicka A, Zlotorowicz A, Kulesza P J. Elucidation of activity of copper and copper oxide nanomaterials for electrocatalytic and photoelectrochemical reduction of carbon dioxide. Current Opinion in Electrochem. 2020. DOI:https://doi.org/10.1016/j.coelec.2020.05.014

[18] Zhou Y, Zhou R, Zhu X, Han N, Song B, Liu T, Hu G, Li Y, Lu J, Li Y. Mesoporous PdAg Nanospheres for Stable Electrochemical CO_2 Reduction to Formate. Advanced Materials. 2020. DOI:https://doi.org/10.1002/adma.202000992

[19] Barcelo G, Sarret M, Müller C, Pregonas J. Corrosion resistance and mechanical properties of zinc electrocoatings. Electrochimical Acta. 1998;43:13-20.

[20] Bowden C, Matthews A. A study of the corrosion properties of PVD Zn-Ni coatings. Surface and Coatings Technology. 1995;76:508-515.

[21] Conde A, Arenas M, De Damborenea J. Electrodeposition of Zn–Ni coatings as Cd replacement for corrosion protection of high strength steel. Corrosion Science. 2011;53:1489-1497.

[22] Beheshti M, Ismail MC, Kakooei S, Shahrestani S. Influence of temperature and potential range on Zn-Ni deposition properties formed by cyclic voltammetry electrodeposition in chloride bath solution. Corrosion Reviews.2020;38(2):127-136. DOI: https://doi.org/10.1515/corrrev-2019-0086

[23] Lin Zf, Li Xb, Xu Lk. Electro-deposition and corrosion behavior of zinc–nickel films obtained from acid solutions: effects of TEOS as additive. International Journal of Electrochemistry science. 2012;7:12507-12517.

[24] Beheshti M, Ismail MC, Kakooei S, Shahrestani S, Mohan G, Zabihiazadboni M. Influence of deposition temperature on the corrosion resistance of electrodeposited zinc-nickel alloy coatings. Materialwissenschaft und Werkstofftechnik. 2018;49(4):472-482. DOI: https://doi.org/10.1002/mawe.201700284

[25] Byk T, Gaevskaya T, Tsybulskaya L. Effect of electrodeposition conditions on the composition, microstructure, and corrosion resistance of Zn–Ni alloy coatings. Surface and Coatings Technology. 2008;202:5817-5823.

[26] D'Alessandro DM, Smit B, Long JR. Carbon dioxide capture: prospects for new materials. Angewandte Chemie International Edition, 2010;49:6058-6082.

[27] Hori Y. Electrochemical CO_2 reduction on metal electrodes. In: Modern Aspects of Electrochemistry. Heidelberg: Springer; 2008. 89-189 pp.

[28] Qiao JL, Liu YY, Hong F, Zhang JJ. A review of catalysts for the electroreduction of carbon dioxide to produce low-carbon fuels. Chemical Society Reviews. 2014;43:631-675.

[29] Jhong HR, Ma S, Kenis PJ. Electrochemical conversion of CO_2 to useful chemicals: current status, remaining challenges, and future opportunities. Current Opinion in Chemical Engineering. 2013;2:191-199.

[30] Lee J, Kwon Y, Machunda RL, Lee HJ. Electrocatalytic recycling of CO_2 and small organic molecules. Asian Journal of Chemistry, 2009;4:1516-1523.

[31] Durand WJ, Peterson AA, Studt F, Abild-Pedersen F, Nørskov JK. Structure effects on the energetics of the electrochemical reduction of CO_2 by copper surfaces. Surface Science. 2011;605:1354-1359.

[32] Hansen HA, Montoya JH, Zhang YJ, Shi C, Peterson AA, Nørskov JK. Electroreduction of methanediol on copper. Catalysis Letters. 2013;143:631-635.

[33] Peterson AA, Abild-Pedersen F, Studt F, Rossmeisl J, Nørskov JK. How copper catalyzes the electroreduction of carbon dioxide into hydrocarbon fuels. Energy and Environmental Sciences. 2010;3:1311-1315.

[34] Peterson AA, Nørskov JK. Activity descriptors for CO_2 electroreduction to methane on transition-metal catalysts. The Journal of Physical Chemistry Letters. 2012;3:251-258.

[35] Cui C, Wang H, Zhu X, Han J, Ge Q. A DFT study of CO_2 electrochemical reduction on Pb(211) and Sn(112). Science China Press and Springer-Verlag Berlin Heidelberg. 2015;58(4):607-613.

[36] Lu Q, Jiao F. Electrochemical CO_2 reduction: Electrocatalyst, reaction mechanism, and process engineering. Nano Energy. 2016;4-9:2211-2855.

[37] Hirunsit P. Electroreduction of carbon dioxide to methane on copper, copper-silver, and copper-gold catalysts: a DFT study Journal of Physical Chemistry C. 2013;117: 8262-8268.

[38] Nie X, Esopi MR, Janik MJ, Asthagiri A. Selectivity of CO_2 reduction on copper electrodes: the role of the kinetics of elementary steps. Angewandte Chemie International Edition. 2013;52:2459-2462.

[39] Nie X, Luo W, Janik MJ, Asthagiri A. Reaction mechanisms of CO_2 electrochemical reduction on Cu (111) determined with density functional theory. Journal of Catalyst. 2014;312:108-122.

[40] Chen Y, Li CW, Kanan MW. Aqueous CO_2 Reduction at Very Low Overpotential on Oxide-Derived Au Nanoparticles. Journal of the American Chemical Society. 2012;134(49):19969-19972.

[41] Rosen J, Hutchings GS, Lu Q, Rivera S, Zhou Y, Vlachos DG, Jiao F. Mechanistic Insights into the Electrochemical Reduction of CO_2 to CO on Nanostructured Ag Surfaces. ACS Catalysis. 2015;5(7):4293-4299.

[42] Nursanto EB, Jeon HS, Kim C, Jee MS, Koh JH, Hwang YJ, Min BK. Gold catalyst reactivity for CO_2 electroreduction: From nano particle to layer. Catalysis Today. 2016;260:107-111.

[43] Jee MS, Jeon HS, Kim C, Lee H, Koh JH, Cho J, Min BK, Hwang YJ. Enhancement in carbon dioxide activity and stability on nanostructured silver electrode and the role of oxygen. Applied Catalysis B. 2016;180:372-378.

[44] Hori Y, Vayenas CG, White RE, Gamboa-Aldeco ME. Electrochemical CO_2 Reduction on Metal Electrodes. MOD. ASPECT. ELECTROC. 2008;42: 89-104.

[45] Quan F, Zhong D, Song H, Jia F, Zhang L. A highly efficient zinc catalyst for selective electroreduction of carbon dioxide in aqueous NaCl solution. Journal of Materials Chemistry A. 2015;3(32):16409-16413.

[46] Rosen J, Hutchings GS, Lu Q, Forest RV, Moore A, Jiao F. Electrodeposited Zn Dendrites with Enhanced CO Selectivity for Electrocatalytic CO_2 Reduction. ACS Catalysis. 2015;5(8):4586-4591.

[47] Won DH, Shin H, Koh J, Chung J, Lee HS, Kim H, Woo SI. Highly Efficient, Selective, and Stable CO_2 Electroreduction on a Hexagonal Zn Catalyst. Angewandte Chemie International Edition. 2016;55(32):9297-9300.

[48] Nguyen DLT, Jee MS, Won DH, Jung H, Oh HS, Min BK, Hwang YJ. Selective CO_2 Reduction on Zinc Electrocatalyst: The Effect of Zinc Oxidation State Induced by Pretreatment Environment. ACS Sustainable Chemistry & Engineering. 2017;5:11377-11386.

[49] Keerthiga G, Chetty R. Electrochemical Reduction of Carbon Dioxide on Zinc-Modified Copper Electrodes. Journal of the Electrochemical Society. 2017;164(4):H164-H169.

[50] Hori Y, Murata A. Electrochemical evidence of intermediate formation of adsorbed CO in cathodic reduction of CO_2 at a nickel electrode. Electrochim. Acta. 1990;35:1777-1780.

[51] Murata A, Hori Y. Electrochemical reduction of CO_2 to CO at Ni electrodesmodified with CD. Chemical Letter. 1991:181-184.

[52] Hori Y, Kikuchi K, Suzuki S. Production of CO and CH_4 in electrochemicalreduction of CO_2 at metal–electrodes in aqueous hydrogencarbonatesolution. Chemical Letter. 1985:1695-1698.

[53] Taguchi S, Aramata A. Surface-structure sensitive reduced CO_2 formationon Pt single crystal electrodes in sulfuric acid solution. Electrochimical Acta, 1994;39:2533-2537.

[54] Kumar B, Brian JP, Atla V, Kumari S, Bertram KA, White RT, Spurgeon JM. New trends in the development of heterogeneous catalysts for electrochemical CO_2 reduction. Catalysis Today. 2016;270:19-30.

[55] Jhong HRM, Ma S, Kenis PJ. Electrochemical conversion of CO_2 to useful chemicals: current status, remaining challenges, and future opportunities. Current Opinion in Chemical Engineering. 2013;2(2): 191-199.

[56] Jhong HR, Brushett FR, Yin L, Stevenson DM, Kenis PJA. Combining Structural and Electrochemical Analysis of Electrodes Using Micro-Computed Tomography and a Microfluidic Fuel Cell. Journal of Electrochemical Society. 2012;159(3):292-298.

[57] Cindrella L, Kannan AM, Lin JF, Saminathan K, Ho Y, Lin CW, Wertz J. Gas diffusion layer for proton exchange membrane fuel cells—A review. PowerSources. 2009;194:146-160.

[58] Furuya N, Yamazaki T, Shibata M. High performance Ru/Pd catalysts for CO_2 reduction at gas-diffusion electrodes. Journal of Electroanalytical Chemistry. 1997;431:39-41.

[59] Rosen BA, Zhu W, Kaul G, Khojin AS, Masel RI. Water Enhancement of CO_2 Conversion on Silver in 1-Ethyl-3-Methylimidazolium Tetrafluoroborate. Journal of Electrochemical Society. 2013;160:138-141.

[60] Rosen BA, Khojin AS, Thorson MR, Zhu W, Whipple DT, Kenis PJA, Masel RI. Ionic Liquid–Mediated Selective Conversion of CO_2 to CO at Low Overpotentials. Science. 2011;334:643-644.

[61] Ramos JM, Pupillo RC, Keane TP, DiMeglio JL, Rosenthal J. Efficient Conversion of CO_2 to CO Using Tin and Other Inexpensive and Easily Prepared Post-Transition Metal Catalysts. Journal of the American Chemical Society. 2015;137:5021-5027.

[62] Asadi M, Kumar B, Behranginia A, Rosen BA, Baskin A, Repnin N, Pisasale D, Phillips P, Zhu W, Haasch R, Klie RF, Kra'l P, Abiade J, Khojin AS. Robust carbon dioxide reduction on molybdenum disulphide edges. Nature Communications. 2014;5:1-8.

[63] Oh Y, Vrubel H, Guidoux S, Hu X. Efficient Reduction of CO_2 to CO with High Current Density Using in Situ or ex Situ Prepared Bi-Based Materials. Chemical Communications. 2014;50:3878-3881.

[64] Oh Y, Hu X. Ionic liquids enhance the electrochemical CO_2 reduction catalyzed by MoO_2. Chemical Communications. 2015;51:13698-13701.

[65] DiMeglio JL, Rosenthal J. Selective Conversion of CO_2 to CO with High Efficiency Using an Inexpensive Bismuth-Based Electrocatalyst. Journal of the American Chemical Society. 2013;135:8798-8801.

[66] Ganesh I, Kumar PP, Annapoorna I, Sumliner JM, Ramakrishna M, Hebalkar NY, Padmanabham G, Sundararajan G. Preparation and characterization of Cu-doped TiO_2 materials for electrochemical, photoelectrochemical, and photocatalytic applications. Applied Surface Science. 2014;293:229-247.

[67] Genovese C, Ampelli C, Perathoner S, Centi G. Electrocatalytic conversion of CO_2 on carbon nanotube-based electrodes for producing solar fuels. Journal of catalyst. 2013;308: 237-249.

[68] Bernstein NJ, Akhade SA, Janik MJ. Density functional theory study of carbon dioxide electrochemical reduction on the Fe(100) surface. Physical Chemistry Chemical Physics. 2014;16:13708-13717.

[69] Friebel D, Mbuga F, Rajasekaran S, Miller DJ, Ogasawara H, Alonso -Mori R, Sokaras D, Nordlund D, Weng TC, Nilsson A. Structure, redox chemistry, and interfacial alloy formation in monolayer and multilayer Cu/Au(111) model catalysts for CO_2 electroreduction. The Journal of Physical Chemistry C. 2014;118:7954-7961.

[70] Terunuma Y, Saitoh A, Momose Y. Relationship between hydrocarbon production in the electrochemical reduction of CO_2 and the characteristics of the Cu electrode. Journal of Electroanalytical Chemistry. 1997;434: 69-75.

[71] Goncalves M., Gomes A, Condeco J, Fernandes R, Pardal T, Sequeira C, Branco J. Selective electrochemical conversion of CO_2 to C_2 hydrocarbons. Energy Convers Manage. 2010;51: 30-32.

[72] Schouten KJP, Kwon Y, van der Ham CJM., Qin Z, Koper MTM. A new mechanism for the selectivity to C-1 and C-2 species in the electrochemical reduction of carbon dioxide on copper electrodes. Chemical Science. 2011;2:1902-1909.

[73] Hori Y, Takahashi I, Koga O, Hoshi N. Selective formation of C_2 compounds from electrochemical reduction of CO_2 at a series of copper single crystal electrodes. Journal of Physical Chemistry B. 2002;106:15-17.

[74] Hori Y, Konishi H, Futamura T, Murata A, Koga O, Sakurai H, Oguma K. Deactivation of copper electrode" in electrochemical reduction of CO_2, Electrochimical Acta. 2005;50: 5354-5369.

[75] Fukatsu A, Kondo M, Okabe Y, Masaoka S. porphyrin-catalyzed CO_2 reduction under photoirradiation. Journal

of Photochemistry and Photobiology A: Chemistry. 2015;313:143-148.

[76] Yang W, Dastafkan K, Jia C, Zhao C. Design of Electrocatalysts and Electrochemical Cells for Carbon Dioxide Reduction Reactions. Advanced Material Technology. 2018;1700377. DOI: 10.1002/admt.201700377

[77] Torelli DA, Francis SA, Crompton JC, Javier A, Thompson JR, Brunschwig BS, Soriaga MP, Lewis NS. Nickel-Gallium-Catalyzed Electrochemical Reduction of CO₂ to Highly Reduced Products at Low Overpotentials. ACS Catalysis. 2016; 6(3):2100-2104.

[78] Ampelli C, Genovese C, Perathoner S, Centi G, Errahali M, Gatti G, Marchese L. An Electrochemical Reactor for the CO₂ Reduction in Gas Phase by Using Conductive Polymer Based Electrocatalysts. Chemical Engineering Transactions. 2014;41:13-18. DOI: 10.3303/cet 1441003,

[79] Mignard D, Barik RC, Bharadwaj AS, Pritchard CL, Ragnoli M, Cecconi F, Miller H, Yellowlees LJ. Revisiting strontium-doped lanthanum cuprate perovskite for the electrochemical reduction of CO₂. Journal of CO₂ Utilization. 2014;5:53-59.

[80] Ullah N, Ali I, Jansen M, Omanovic S. Electrochemical Reduction of CO₂ in an Aqueous Electrolyte Employing an Iridium/Ruthenium-Oxide Electrode. Canadian Journal of Chemical Engineering. 2015;93:55-62. DOI 10.1002/cjce.22110,

[81] Guo X, Zhang Y, Deng C, Li X, Xue Y, Yan YM, Sun K. Composition dependent activity of Cu–Pt nanocrystals for electrochemical reduction of CO₂. Chem. Commun. 2015;51:1345-1352.

[82] Maark TA, Nanda BRK. CO and CO₂ Electrochemical Reduction to Methane on Cu, Ni, and Cu₃Ni (211) Surfaces. J. Phys. Chem. C. 2016;120:8781-8789.

[83] Pérez-Rodrígueza S, Rilloa N, Lázaroa MJ, Pastor E. Pd catalysts supported onto nanostructured carbon materials for CO₂ valorization by electrochemical reduction. Applied Catalysis B: Environmental. 2015;163:83-95.

[84] Bellini M, Folliero MG, Evangelisti C, He Q , Hu Yf, Pagliaro MV, Oberhauser W, Marchionni A, Filippi J, Miller HA, Vizza F. A Gold-Palladium Nanoparticle Alloy Catalyst for CO Production from CO₂ Electroreduction. Energy Technology. 2018.https://doi.org/10.1002/ente.201800859

[85] Grote JP, Zeradjanin AR, Cherevko S, Savan A, Breitbach B, Ludwig A, Mayrhofer KJJ. Screening of material libraries for electrochemical CO₂ reduction catalysts – Improving selectivity of Cu by mixing with Co. Journal of Catalysis.2016;343:248-256.

[86] Ma M, Hansen HA, Valenti M, Wang Z, Cao A, Dong M, Smith WA. Electrochemical reduction of CO₂ on compositionally variant Au-Pt bimetallic thin films. Nano Energy. 2017; 42:51-57.

[87] Choi J, Kim MJ, Ahn SH, Choi I, Jang JH, Ham YS, Kim JJ, Kim SK. Electrochemical CO₂ reduction to CO on dendritic Ag–Cu electrocatalysts prepared by electrodeposition. Chemical Engineering Journal, 2016; 299:37-44.

[88] Zhu Q , Ma J, Kang X, Sun X, Hu J, Yang G, Han B. Electrochemical reduction of CO₂ to CO using graphene oxide/carbon nanotube electrode in ionic liquid/acetonitrile system., Chemistry. 2016;59-5: 551-556. doi: 10.1007/s11426-016-5584-1

[89] Aeshala LM, Uppaluri RG, Verma A. Effect of cationic and anionic solid polymer electrolyte on direct electrochemical reduction of gaseous

CO_2 to fuel. Journal of CO_2 Utilization, 2013;3-4:49-55.

[90] Newman J, Thomas-Alyea KE. Electrochemical system. third edition, university of California, Berkeley, Inc publication, Copy write. TP255.N48. 2004.

[91] Velichenko A, Sarret M, Müller C. Nature of the passive film formed at a zinc anode in zinc–nickel containing solutions. Journal of Electroanalytical Chemistry. 1998;448:1-3.

[92] Qiao X, Li H, Zhao W, Li D. Effects of deposition temperature on electrodeposition of zinc–nickel alloy coatings. Electrochimical Acta. 2013;89:771-777.

[93] Baldwin K, Robinson M, Smith C. The corrosion resistance of electrodeposited zinc-nickel alloy coatings. Corrosion science. 1993;35:1267-1272.

[94] Alfantazi A, Brehaut G, Erb U. The effects of substrate material on the microstructure of pulse-plated Zn–Ni alloys. Surface and Coatings Technology. 1997;89:239-244.

[95] El Rehim SA, Fouad E, El Wahab SA, Hassan HH. Electroplating of zinc-nickel binary alloys from acetate baths. Electrochimical Acta. 1996;41:1413-1418.